First stable reduced form of $[Co_5]^{+10}$: fine tuning of linear pentacobalt(II) complexes containing delocalized metal–metal bonds through ligand modification†

Wen-Zhen Wang,[a,b] Rayyat Huseyn Ismayilov,[a,b] Rui-Ren Wang,[a] Yi-Lin Huang,[c] Chen-Yu Yeh,[c] Gene-Hsiang Lee[a] and Shie-Ming Peng*[a,b]

Received 7th July 2008, Accepted 8th September 2008
First published as an Advance Article on the web 22nd October 2008
DOI: 10.1039/b811520f

Pentacobalt EMACs $[Co_5(\mu_5\text{-dpzpda})_4X_2]$ (X = Cl^- (**1**), NCS^- (**2**)) with fine-tuning of the supporting ligand based on the tripyridyldiamine ligand, *N*,*N*′-di(pyrazin-2-yl)pyridine-2,6-diamine (H_2dpzpda), and their reduced form $(Ph_4P)[Co_5(\mu_5\text{-dpzpda})_4X_2]$ (X = Cl^- (**3**), NCS^- (**4**)) were first synthesized and structurally characterized. The structures of **1–4** showed direct Co–Co bonds with Co–Co distances in the range 2.2385(7)–2.2888(15) Å, and valence electrons delocalized through the whole metal chain with distances of longer than 9.06 Å. The distances of the inner Co–Co bonds and the Co–axial ligands became longer after reduction, whereas no significant change was observed in the distances of the outer Co–Co bonds and Co–N (supporting ligand) bonds, which was consistent with the MO analysis. Electrochemical studies on both **1** and **2** showed one reversible oxidation and one reversible reduction at $E_{1/2}$ = +0.82 and –0.05 V for **1**, and at $E_{1/2}$ = +0.89 and +0.02 V for **2**, respectively. The redox reactions of the thiocyanate complex **4** happened at higher potentials than the chloride complex **3**. A magnetism study of **1–4** revealed anomalous magnetic behaviour similar to that of heptacobalt EMACs, and a deviation from the Curie–Weiss law was observed. The $\chi_M T$ value at 300 K is 0.84 and 1.16 emu K mol^{-1} for **1** and **2**, respectively, suggesting spin-equilibrium or a spin-admixture between doublet and quartet states arising from the Boltzmann distribution over different energy levels. Similar results were obtained for **3** and **4**, showing intermediate $\chi_M T$ values between a diamagnetic and a triplet state of 0.15–0.96 emu K mol^{-1} in the temperature range 5–300 K. The structural and magnetic results were interpreted through an EHMO study.

Introduction

A great deal of attention has been paid to metal string complexes, the so-called extended metal atom chain complexes (EMAC) over the past several decades due to their importance in understanding metal–metal interactions in polynuclear systems. Interests in this unique family has been further enhanced by the recent discovery of their potential application as molecular electronic devices due to the study of their electronic conductivity.[1] A large variety of EMACs have been synthesized by our group and Cotton's group, and the metals have been expanded from first row transition metals to some second and even third row transition metals, including Cr,[2] Co,[3] Ni,[4] Cu,[5] Pd,[6] Ru[7] and Rh[7a] Much of the work has focused on EMACs of oligo-α-pyridylamido ligands (Scheme 1), among which metal–metal interactions have been found in cobalt, ruthenium, rhodium, some chromium and oxidized nickel EMACs. The metal–metal interactions are

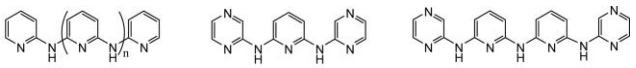

Scheme 1

crucial for electron conductivity as the electron delocalization over the metal chain plays a vital role in electronic transitions, and the redox property involving loss and gain of electrons provides bistable states, which form the base of molecular switches. Investigation *via* STM (scanning tunneling microscopy) revealed that EMACs with metal–metal bonds and delocalized electronic configuration showed better conductivity than those with localized electronic configuration and without metal–metal bonds, and the conductance correlated well with the metal–metal bond order in EMACs.[1a,1c] Cobalt and some chromium EMACs, have exhibited a delocalized structure with marked metal–metal interactions and show promise for use as nanodevices because of their significant conductance. Of particular note, tricobalt EMACs showed both molecules of symmetrical and unsymmetrical structures offering a very rare example of bond-stretch isomers, and all known cobalt EMACs[3a–d] had net Co–Co bonds in their molecules. Previous research on EMACs of oligo-α-pyridylamido ligands has revealed that the strength of the metal–metal interactions is dependent on the type, number and oxidation states of metal centers, and

[a]*Department of Chemistry, National Taiwan University, Taipei, Taiwan, ROC. E-mail: smpeng@ntu.edu.tw*
[b]*Institute of Chemistry, Academia Sinica, Taipei, Taiwan, ROC*
[c]*Department of Chemistry, National Chung Hsing University, Taichung, Taiwan, ROC*

† Electronic supplementary information (ESI) available: Molecular structures of (**3**) and (**4**). CCDC reference numbers 694067–694070. For ESI and crystallographic data in CIF or other electronic format see DOI: 10.1039/b811520f

the nature of the ligands. Therefore more recently, our group has developed a growing interest in the fine modification of spacer ligands. Over the past several years, a series of tuning oligo-α-pyridylamido ligands, modified with pyrazine, naphthyridine and toluenesulfonyl *etc.,* instead of pyridine rings have been designed and synthesized. The resultant EMACs showed encouraging changes in molecular energy levels with resultant changes in redox and magnetic properties of the complexes.

The magnetism of cobalt EMACs is also a particularly fascinating topic. Tricobalt EMACs of both s- and u-$[Co_3(dpa)_4Cl_2]$ (Hdpa = di(2-pyridyl)amine) showed a doublet ground state at low temperature, and both underwent spin crossover as the temperature was increased. Some tricobalt EMACs experienced a two-step spin crossover to $S = 3/2$ and $5/2$ states.[3a] The pentacobalt EMAC $[Co_5(tpda)_4(NCS)_2]$ (H_2tpda = tripyridyldiamine) had a doublet ground state with a temperature-independent magnetic moment. A triplet ground state was observed when the compound underwent one-electron oxidation.[3b] Using pyrazine-modulated ligands N^2-(pyrazin-2-yl)-N^6-(6-(pyrazin-2-ylamino)pyridin-2-yl)pyridine-2,6-diamine (H_3pzpz) (Scheme 1) and *N,N*-[6-(pyrazin-2-ylamino)pyridin-2-yl,pyridin-2-yl]pyridine-2,6-diamine (H_3tpz), heptacobalt EMACs $[Co_7(\mu_7\text{-}L)_4X_2]$ ($L = pzpz^{3-}$, tpz^{3-}; $X = Cl^-$, NCS^-) were obtained and spin-equilibrium was formed in this series, which resulted in intermediate magnetic moments between doublet and quartet spin states and a slow decrease in the values upon cooling.[3d] With such abundant magnetic behaviour and unique molecular and electronic structure, cobalt EMACs are one of the most challenging systems to investigate.[8] However, the number of cobalt EMACs are extremely limited and the study of them remains scarce due to the synthetic difficulties. In order to get more insight into the electronic structure and magnetic properties of cobalt EMACs, we designed a pyrazine-modulated tripyridyldiamine ligand, *N*,*N*′-di(pyrazin-2-yl)pyridine-2,6-diamine (H_2dpzpda) (Scheme 2).[9] Here we focus on the fine tuning of pentacobalt EMACs, $[Co_5(\mu_5\text{-dpzpda})_4X_2]$ ($X = Cl^-$ (**1**), NCS^- (**2**)) and their reduced form, $(Ph_4P)[Co_5(\mu_5\text{-dpzpda})_4X_2]$ ($X = Cl^-$ (**3**), NCS^- (**4**)) is also reported for the first time, in comparison with previous reports on $[Co_3(dpa)_4X_2]$, $[Co_5(tpda)_4X_2]$ and $[Co_7(\mu_7\text{-}L)_4X_2]$ ($L = pzpz^{3-}$, tpz^{3-}; $X = Cl^-$, NCS^-).

Results and discussion

Syntheses and structures

Complex **1** was synthesized by reacting anhydrous $CoCl_2$ with H_2dpzpda in naphthalene in an argon atmosphere employing Bu^{t}OK to deprotonate the amine group. The thiocyanate complex **2** was obtained by an axial ligand exchanging reaction from **1**. The treatment of **1** and **2** with hydrazine afforded the one-electron reduced species, **3** and **4**, respectively (Scheme 2). This is the first example of reduced EMACs for non-naphthyridine-modulated oligo-α-pyridylamido ligands. Complexes **1** and **2** are fairly stable, whereas **3** and **4** are air-sensitive and could undergo spontaneous oxidation in air forming **1** and **2**. Thus, all the physical measurements for **3** and **4** were applied to freshly prepared samples.

The crystal data for **1–4** are listed in Table 1 and the selected bond lengths and angles are listed in Table 2. A comparison of the

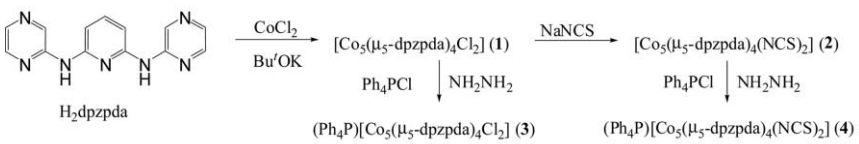

Scheme 2

Table 1 Crystal data for **1–4**

	1·4CHCl$_3$	**2**·4CH$_2$Cl$_2$	**3**·2CH$_2$Cl$_2$·2H$_2$O	**4**·4CH$_2$Cl$_2$
Formula	$C_{56}H_{40}Cl_{14}Co_5N_{28}$	$C_{58}H_{44}Cl_8Co_5N_{30}S_2$	$C_{78}H_{64}Cl_6Co_5N_{28}O_2P$	$C_{82}H_{64}Cl_8Co_5N_{30}PS_2$
Formula weight	1896.11	1803.60	1963.89	2142.97
Crystal system	Orthorhombic	Orthorhombic	Monoclinic	Triclinic
Space group	*Pbca*	*Pbcn*	*C*2/*c*	$P\bar{1}$
a/Å	22.6213(4)	12.2216(8)	16.3673(7)	14.8060(4)
b/Å	12.8225(2)	21.3254(15)	27.5890(14)	16.8778(4)
c/Å	24.5904(4)	26.4776(17)	17.3331(8)	17.7166(5)
α/°	90	90	90	98.6556(15)
β/°	90	90	91.231(3)	93.3470(14)
γ/°	90	90	90	90.8523(16)
V/Å^3	7132.7(2)	6900.9(8)	7825.1(6)	4368.1(2)
Z	4	4	4	2
D_c/Mg m^{-3}	1.766	1.736	1.667	1.629
Absorption coefficient/mm^{-1}	1.725	1.613	1.333	1.306
Crystal size/mm	0.02 × 0.14 × 0.38	0.15 × 0.12 × 0.10	0.32 × 0.20 × 0.01	0.20 × 0.14 × 0.03
θ range for data collection/°	1.66–27.50	1.54–25.00	1.45–25.00	1.55–27.50
Reflection collected	47 098	27 749	14 150	65 266
Independent reflections	8193 (R_{int} = 0.0701)	6079 (R_{int} = 0.1089)	6830 (R_{int} = 0.0357)	19869 (R_{int} = 0.0641)
R_1, wR_2 (F^2) ($I > 2\sigma(I)$)	0.0630, 0.1491	0.0534, 0.1133	0.0739, 0.2129	0.0728, 0.1868
R_1, wR_2 (F^2) (all data)	0.1040, 0.1660	0.1383, 0.1433	0.0929, 0.2313	0.1405, 0.2226
GOF	1.001	1.030	1.046	1.010

Table 2 Selected bond distances (Å) and angles (°) for **1–4**[d]

Complex	1	2	3	4
Co(1)–Co(2)	2.2865(9)	2.2793(10)	2.2888(15)	2.2830(10)
Co(2)–Co(3)	2.2449(6)	2.2385(7)	2.2793(15)	2.2582(10)
Co(3)–Co(4)[a]	2.2449(6)	2.2385(7)	2.2745(15)	2.2582(10)
Co(4)–Co(5)[a]	2.2865(9)	2.2793(10)	2.2867(15)	2.2803(10)
Co(1)–N[b]	1.972(5)	1.968(4)	1.964(5)	1.964(5)
Co(2)–N[b]	1.912(9)	1.912(4)	1.918(5)	1.916(4)
Co(3)–N[b]	1.938(4)	1.937(6)	1.944(5)	1.936(5)
Co(4)–N[a,b]	1.912(9)	1.912(4)	1.924(5)	1.917(5)
Co(5)–N[a,b]	1.972(5)	1.968(4)	1.968(5)	1.970(5)
Co(1)–X[c]	2.4062(15)	2.040(5)	2.450(2)	2.106(5)
Co(5)–X[a,c]	2.4062(15)	2.040(5)	2.484(3)	2.093(5)
N(1)–C(1)[b,d]	1.333(14)	1.348(7)	1.357(9)	1.354(7)
N(1)–C(4)[b,d]	1.378(12)	1.358(7)	1.363(8)	1.365(7)
N(2)–C(4)[b,d]	1.487(13)	1.362(7)	1.357(8)	1.358(7)
N(2)–C(5)[b,d]	1.503(13)	1.390(7)	1.383(8)	1.380(7)
N(3)–C(5)[b,d]	1.364(11)	1.370(6)	1.371(7)	1.366(7)
N(6)–C(2)[b,d]	1.414(20)	1.340(7)	1.351(10)	1.350(9)
N(6)–C(3)[b,d]	1.300(20)	1.319(7)	1.318(9)	1.315(8)
C(1)–C(2)[b,d]	1.368(19)	1.370(8)	1.363(10)	1.354(7)
C(3)–C(4)[b,d]	1.421(16)	1.421(8)	1.423(9)	1.417(9)
C(5)–C(6)[b,d]	1.403(16)	1.389(7)	1.398(9)	1.389(8)
C(6)–C(7)[b,d]	1.381(13)	1.375(7)	1.379(9)	1.386(9)
X[c]–Co(1)–Co(2)	179.16(6)	179.67(13)	180.0	179.20(14)
Co(1)–Co(2)–Co(3)	178.95(4)	179.16(5)	180.0	179.42(5)
Co(2)–Co(3)–Co(4)[a]	180.0	179.80(6)	180.0	179.91(5)
Co(3)–Co(4)–Co(5)[a]	178.95(4)	179.16(5)	180.0	179.78(5)
Co(4)–Co(5)–X[a,c]	179.16(6)	179.67(13)	180.0	179.33(15)
N–Co(1)–Co(2)–N[b]	25.77	24.42	23.94	23.49
N–Co(2)–Co(3)–N[b]	19.00	19.98	17.50	19.31
N–Co(1)–Co(5)–N[a,b]	90.00	88.39	82.86	85.59

[a] Co(4) = Co(2A) and Co(5) = Co(1A) for **1** and **2**. Symmetry codes for **1**, A = $-x$, $-y+1$, $-z+1$; for **2**, A = $-x$, y, $-z+1/2$. [b] Average value from the four wrapping ligands. [c] X = Cl^- for **1** and **3**, X = N from NCS^- for **2** and **4**. [d] Data were calculated based on the label in Scheme 4.

Co–Co and Co–N distances among the pentacobalt(II) complexes is shown in Scheme 3.

Both **1** and **2** are neutral complexes, and their structures are similar to those of $[Co_5(\mu_5\text{-tpda})_4X_2]$ (X = Cl^-, NCS^-), showing an EMAC structure with four deprotonated supporting ligands $dpzpda^{2-}$ wrapped around the linear metal chain in a *syn–syn* form as dianion helices, as seen in Fig. 1 and 2.[3b] Two chloride or thiocyanate anions bond to the terminal metal as axial ligands, and the chloride or nitrogen atoms of NCS^- are co-linear with the Co_5 metal score chain. In complex **1**, there is a 2-fold axis perpendicular to the metal chain, and two of the four supporting $dpzpda^{2-}$ ligands in **1** are disordered to two equally occupied positions. In complex **2**, the Co(3) atom sits on a symmetrical center. The Co–Co–Co angles are in the range 178.95–180.0°. The torsion angles for adjacent Co(II) are between 19.00–25.77°, and the average value for the total torsion angles for one ligand, *i.e.* N–Co(1)–Co(5)–N is 90.00 and 88.39° for **1** and **2**, respectively, which is consistent with the previously reported results for EMACs of oligo-α-pyridylamido ligands.[2b,3d] The whole length of the Co_5 chain is about 9.04 and 9.06 Å for **1** and **2**, respectively. The Co–Co distances for **1** and **2** lie in the range 2.2385(7)–2.2865(9) Å, indicating fully delocalized metal–metal bonds through the Co_5 metal chain. In both complexes, the external bonds (Co(1)–Co(2)) are longer than the internal bonds (Co(2)–Co(3)) due to the effects of the axial ligands. The Co(1)–Co(2) and Co(1)–N distances in **1** are longer than those in **2**, because Cl^- provides a stronger ligand field than NCS^-. All Co–N distances lie in the range 1.910(9)–1.975(5) Å with the Co(2)–N bond distances being shorter than Co(1)–N and Co(3)–N bond distances, since the negative density on amido nitrogen atoms (N(2)) is higher than that on the pyrazyl or pyridyl nitrogen atoms (N(1) and N(3)) (Scheme 4). The Co–Cl distance in **1** (2.4062(15) Å) and the Co–N(NCS) distance in **2** (2.040(5) Å) are short in comparison with $[Co_5(\mu_5\text{-tpda})_4Cl_2]$ (2.445(2) Å) and $[Co_5(\mu_5\text{-tpda})_4(NCS)_2]$ (average 2.073(8) Å) (Scheme 3).[3b]

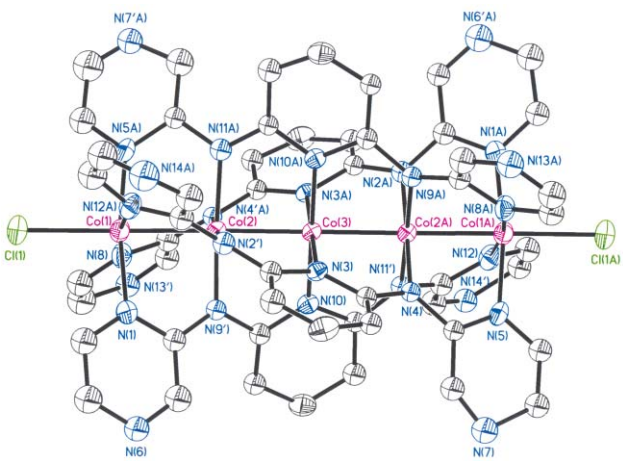

Fig. 1 The molecular structure of $[Co_5(\mu_5\text{-dpzpda})_4Cl_2]$ (**1**). Atoms are drawn at the 50% probability level. Disordered atomic positions and hydrogen atoms are omitted for clarity. Label A was generated through the symmetry operation ($-x$, $-y+1$, $-z+1$).

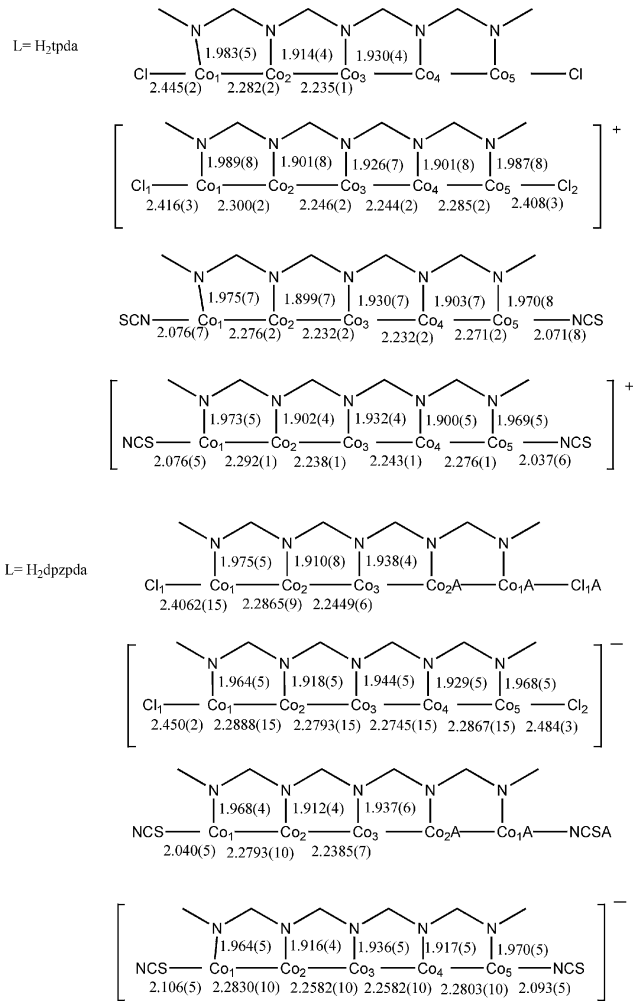

Scheme 3 Comparison of bond distances in pentacobalt(II) EMAC complexes. Data for complexes of H_2tpda were taken from ref. 3b.

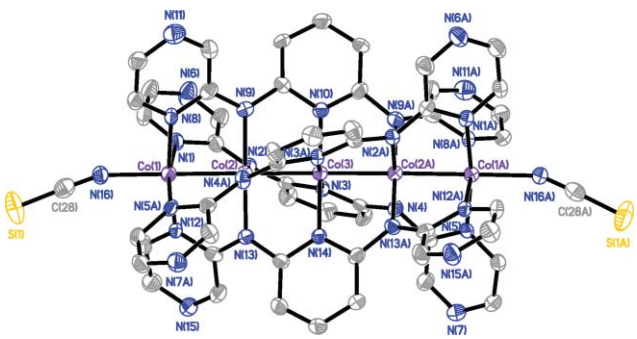

Fig. 2 The molecular structure of $[Co_5(\mu_5\text{-dpzpda})_4(NCS)_2]$ (**2**). Atoms are drawn at the 50% probability level. Hydrogen atoms are omitted for clarity. Label A was generated through the symmetry operation ($-x$, y, $-z + 1/2$).

The one-electron reduced species **3** and **4**, are anionic complexes containing one $(Ph_4P)^+$ as the counter cation in each molecule. The complex anion maintains the same EMAC structure as its precursor complexes **1** and **2**, respectively (Fig. 3 and 4 and ESI, Fig. S1 and S2†). The molecular chain of **3** resides on a 2-fold axis symmetry, thus the metal chain of **3** is a strict line defined by crystallographic symmetry. The Co–Co–Co angles for **4** are

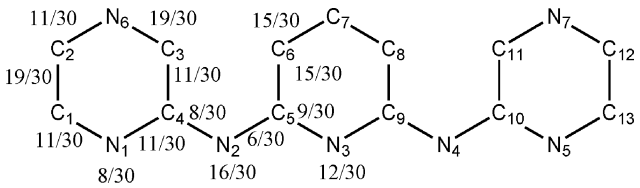

Scheme 4 Negative charge distribution and π bond orders of the ligand anion, $dpzpda^{2-}$.

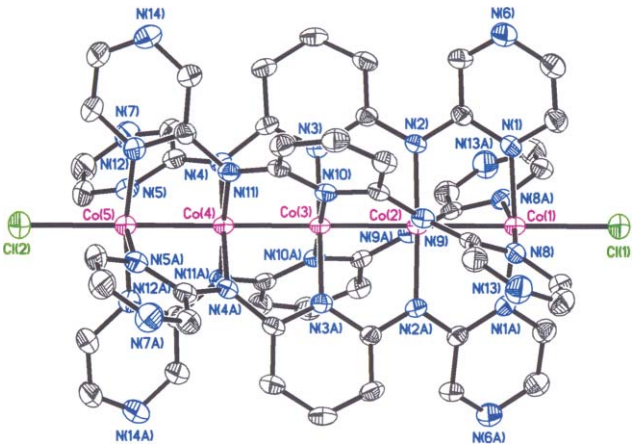

Fig. 3 The molecular structure of the anion in $(Ph_4P)[Co_5(\mu_5\text{-dpzpda})_4Cl_2]$ (**3**). Atoms are drawn at the 50% probability level. Hydrogen atoms are omitted for clarity. Label A was generated through the symmetry operation ($-x + 1$, y, $-z + 3/2$).

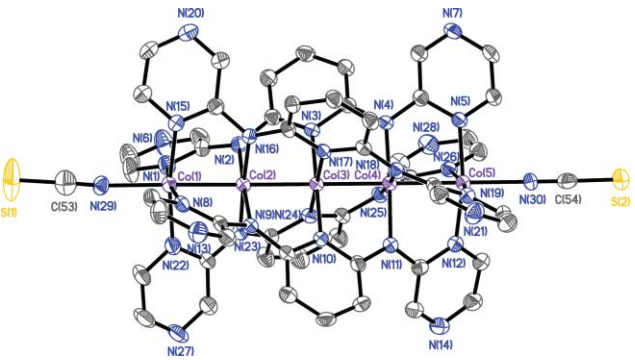

Fig. 4 The molecular structure of the anion in $(Ph_4P)[Co_5(\mu_5\text{-dpzpda})_4(NCS)_2]$ (**4**). Atoms are drawn at the 50% probability level. Hydrogen atoms are omitted for clarity.

in the range 179.42–179.91°. The Co–Co distances for **3** and **4**, in the range 2.2582(10)–2.2888(15) Å, revealed the existence of cobalt–cobalt bonds, which are fully delocalized through the Co_5 metal chain. The Co(1)–Co(2) distances and Co–N distances for **3** and **4** remain essentially unchanged upon one-electron reduction. However, the Co(2)–Co(3) distances in **3** and **4** are significantly longer than those in **1** and **2**, and the Co–Cl distances in **3** (average 2.467(3) Å) and Co–N(NCS) distances in **4** (average 2.099(5) Å) are also longer than those in **1** and **2**. The torsion angles for adjacent Co(II) and total torsion angles for one ligand of **3** and **4** are both slightly smaller than those of **1** and **2**.

Scheme 4 shows the charge distributions and π bond orders of the ligand anion $dpzpda^{2-}$. The calculation was based on resonance

analysis by restraining negative charges on the coordinated nitrogen atoms for simplification. The bond distances of **1–4** are consistent with the calculation results. (1) The negative densities on the amido nitrogen atoms (N(2) and N(4)) are higher than those on the pyridyl nitrogen atoms (N(1), N(3) and N(5)), and consequently the Co–N_{amido} bonds are stronger than Co–$N_{pyridyl}$ bonds and the former bond distances are shorter than the latter (Table 2 and Scheme 3). The terminal nitrogen atom has the least negative charge, and the terminal Co(1)–N bond lengths are the longest. (2) Among all C–C bonds, the π bond order decreased in the order: C(1)–C(2) (19/30), C(5)–C(6) (15/30), and C(3)–C(4) (11/30). In all complexes, the C–C bond distances increased in the same order, indicating that the strongest π bond character is between C(1)–C(2) and the weakest is between C(3)–C(4). (3) The same phenomena was observed for N–C bonds; the highest π bond order among all N–C bonds was N(6)–C(3) (19/30), which showed the shortest bond distance. N(2)–C(4), N(2)–C(5) and N(3)–C(5) had a relatively low π bond order (6/30–9/30), and their distances were comparably longer.

Electrochemistry

The cyclic voltammograms of complexes **1** and **2** were measured in solutions of CH_2Cl_2 in the range −1.6 to +1.6 V, and showed two reversible, one-electron redox couples at $E_{1/2}$ = +0.82 and −0.05 V for **1**, and at $E_{1/2}$ = +0.89 and +0.02 V for **2**, respectively (Fig. 5). A slightly anodical shift was observed when the axial chloride ligands were replaced by thiocyanate, as found for other EMACs.[10] The CV data are summarized in Table 3.

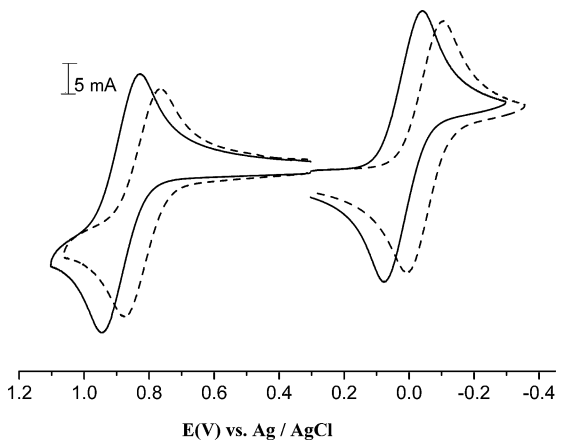

Fig. 5 Cyclic voltammograms of pentacobalt(II) EMACs **1** (dashed lines) and **2** (solid lines) in CH_2Cl_2 containing 0.1 M TBAP.

In order to determine the oxidation states at potentials −0.05 V for **1** and +0.02 V for **2**, spectroelectrochemical techniques were employed on **1** and **2** in CH_2Cl_2 containing 0.1 M TBAP (Fig. 6 and 7). Fig. 6 shows the spectral changes of **1** at various applied potentials from +0.10 to −0.17 V. The peaks at 275 and 535 nm decrease, and those at 297, 370, 620, and 755 nm increase as the applied potential increases. The absorption spectrum was restored when the applied potential of −0.17 V was set back to +0.10 V. This indicates that the electrochemical process is reversible and the wave at $E_{1/2}$ = −0.05 V corresponds to the reduction of **1** to form $\mathbf{1}^-$. The clear isosbestic points at 285, 325, 345, 400, 455, 530, 560 and 805 nm indicate that no intermediates were produced during the reduction process. The spectra of **1** after reduction are consistent with the UV-vis absorption spectrum of chemically reduced product, **3**. The oxidation of **1** was also performed at various applied potentials from +0.73 to +0.93 V. The absorption bands at 275, 340, 535 and 600 nm decreased, and those at 390 nm and a broad peak centered at 975 nm in near IR area increased with isosbestic points at 285, 325, 380 and 555 nm. Similar results to **1** were obtained for **2** (Fig. 7), indicating that the redox processes took place in the metal core chain of Co_5.

Table 3 Redox potentials for pentacobalt EMAC complexes

Complex	**1**	**2**	$[Co_5(\mu_5\text{-tpda})_4Cl_2]$[10]	$[Co_5(\mu_5\text{-tpda})_4(NCS)_2]$[10]
$E_{1/2}$(ox.)/V	+0.82	+0.89	+0.34, +0.86, +1.21, +1.34	+0.38, +0.88
$E_{1/2}$(red.)/V	−0.05	+0.02	−0.55[a]	−0.53

[a] Irreversible reaction.

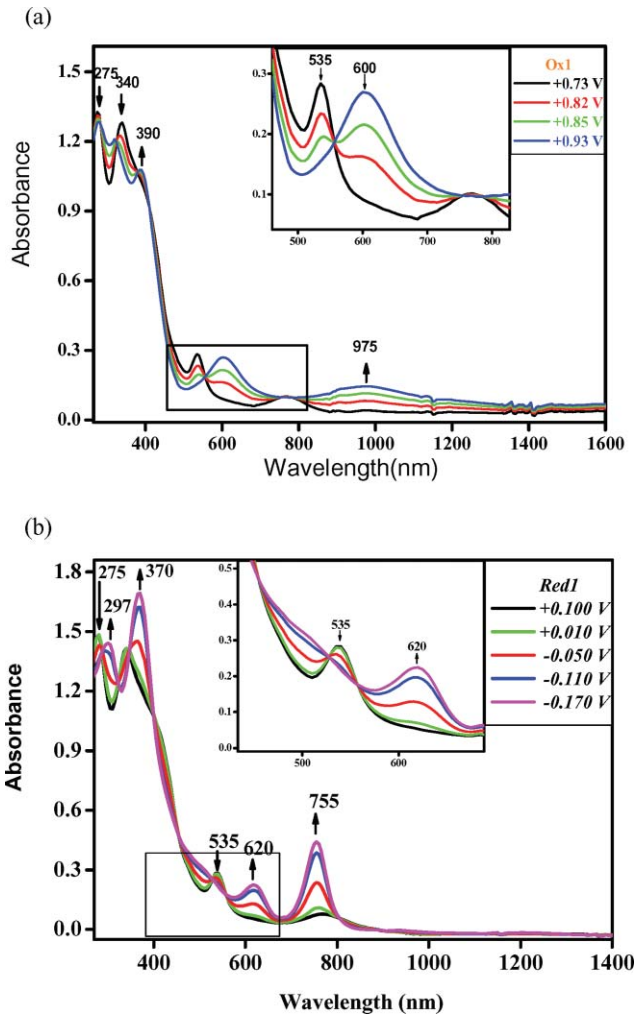

Fig. 6 Spectral changes of $[Co_5(\mu_5\text{-dpzpda})_4Cl_2]$ (**1**) in CH_2Cl_2 with 0.1 M TBAP at various applied potentials (a) from +0.73 to +0.93 V and (b) from +0.10 to −0.17 V, respectively.

These results are strikingly different from the EMAC complexes of the unsubstituted ligand (H_2tpda), $[Co_5(\mu_5\text{-tpda})_4X_2]$

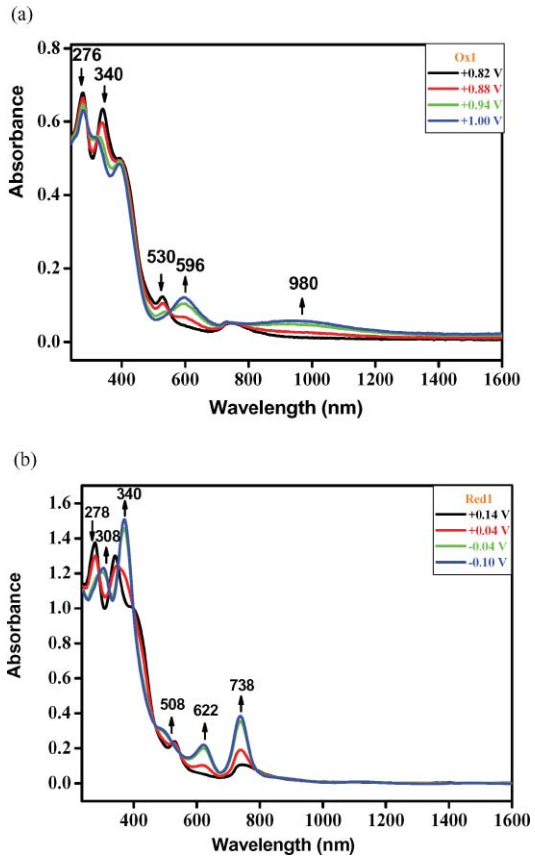

Fig. 7 Spectral changes of $[Co_5(\mu_5\text{-dpzpda})_4(NCS)_2]$ (**2**) in CH_2Cl_2 with 0.1 M TBAP at various applied potentials (a) from +0.82 to +1.00 V and (b) from +0.14 to –0.10 V, respectively.

(X = Cl^-, NCS^-, N_3^- and CN^-).[3b,10] In $[Co_5(\mu_5\text{-tpda})_4X_2]$, 2–4 oxidation peaks and one reduction potential were observed: the first oxidation peak was at +0.34 and +0.38 V, and the reduction potential at –0.55 and –0.53 V for $[Co_5(\mu_5\text{-tpda})_4Cl_2]$ and $[Co_5(\mu_5\text{-tpda})_4(NCS)_2]$, respectively (Table 3). The first oxidation and the reduction potentials of complexes **1** and **2** exhibited an anodical shift of about 0.50 V compared to $[Co_5(\mu_5\text{-tpda})_4Cl_2]$ and $[Co_5(\mu_5\text{-tpda})_4(NCS)_2]$, therefore **1** and **2** showed a much more stable oxidation but could undergo reduction more easily than the corresponding $[Co_5(\mu_5\text{-tpda})_4X_2]$. The introduction of the electron-withdrawing group pyrazine instead of pyridine to the pentacobalt complexes facilitates reduction and retards oxidation, which makes the reduced form of EMACs more accessible and allows us to synthesize **3** and **4** by reducing **1** and **2**, respectively.

Magnetic properties

The magnetic susceptibility of complexes **1** and **2** were measured over a temperature range of 2–300 K and the results are listed in Table 4. The product of the molar magnetic susceptibility and temperature, $\chi_M T$, were depicted as a function of temperature in Fig. 8. For **1** and **2**, the $\chi_M T$ value at 300 K is 0.84 and 1.16 emu K mol^{-1}, respectively. Upon cooling, the $\chi_M T$ decreased gradually to a value of 0.53 and 0.71 emu K mol^{-1} at 2 K for **1** and **2**, respectively. Over the whole temperature range from 2–300 K, **1** and **2** showed $\chi_M T$ values significantly higher than a theoretical spin-only value for a doublet ground state

Table 4 Magnetic data for **1–4**

Complex	**1**	**2**	**3**	**4**
$\chi_M T$ at 300 K/emu K mol^{-1}	0.845	1.160	0.526	0.956
$\chi_M T$ at 2 K/emu K mol^{-1}	0.530	0.709	0.152[a]	0.208

[a] Data measured at 5 K.

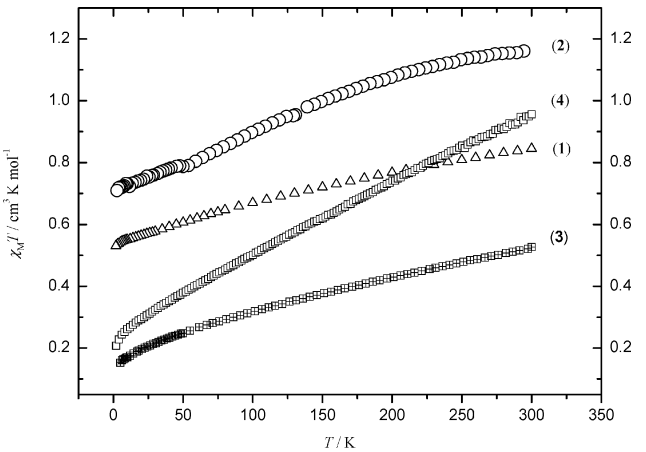

Fig. 8 Experimental $\chi_M T$ values' dependence on temperature from susceptibility data for complexes **1–4**.

(0.38 emu K mol^{-1}) but much lower than that for a quartet ground state (1.88 emu K mol^{-1}). The magnetic behaviour of **1** and **2** is strikingly different from that of the pentacobalt EMAC of unmodulated ligand, $[Co_5(\mu_5\text{-tpda})_4(NCS)_2]$, which showed a doublet ground state with a temperature-independent magnetic moment of 1.93μ_B ($\chi_M T$ value is 0.47 emu K mol^{-1}).[3g] The magnetic behaviour deviated from the Curie–Weiss law, however, no spin crossover phenomenon was observed for **1** and **2** as was the case for the tricobalt EMACs. This anomalous magnetic behaviour, showing intermediate magnetic moment values between doublet and quartet or higher states, is very similar to the pyrazine-modulated hetpacobalt EMACs, and that previously observed in other octahedral cobalt(II) complexes.[3d] Although a large orbital contribution due to spin–orbital coupling is expected for cobalt complexes in some cases, previous research on tricobalt and pentacobalt EMAC analogues, leads us to suggest that we can not attribute such a significant change of $\chi_M T$ value in **1** and **2** (an overall drop of 0.53–0.66 emu K mol^{-1} during temperature measurement), merely to an orbital contribution. It is more reasonable to expect that a spin equilibrium or a spin-admixture arising from the Boltzmann distribution over different energy levels is responsible for the anomalous magnetic behaviour. Due to the formation of fully delocalized Co–Co bonds composed of five cobalt atoms, quite a small energy gap between the HOMO and LUMO is expected, leading to thermally accessible low-lying excited states. Actually, it was found that both the spin states of $S = 3/2$ and $S = 5/2$ were populated in $[Co_3(dpa)_4Cl_2]$, and a minor change to the supporting ligand was able to effect the relative energy of the high-spin state of this type of compound considerably.[3e]

Complexes **3** and **4** gave $\chi_M T$ values at room temperature of 0.53 and 0.96 emu K mol^{-1}, respectively, and these decreased continuously upon cooling to a value of 0.15 emu K mol^{-1} at 5 K

for **3** and 0.21 emu K mol^{-1} at 2 K for **4** (Fig. 8). The $\chi_M T$ values, which were lower than a theoretical spin-only value of a triplet ground state (1.00 emu K mol^{-1}), showed a paramagnetic system and a similar variable-temperature magnetic curve to that of **1** and **2**. It was noticed that the $\chi_M T$ values of both thiocyanates (**2** and **4**) are higher than the corresponding chloride species (**1** and **3**), and the decreasing rate of $\chi_M T$ of both thiocyanate is larger than the chloride species. Because of the electron pairing of the extra electron from reduction, the $\chi_M T$ values of **3** and **4** were 0.20–0.50 emu K mol^{-1} lower than the values of the corresponding initial complexes **1** and **2**. This unusual magnetic behaviour, parallel to that of complexes **1** and **2**, suggests a formation of spin equilibrium or spin-admixture with some orbital contribution from spin–orbital coupling. In the oxidized species $[Co_3(dpa)_4Cl_2][BF_4]$, a two-step spin crossover with spin states of $S = 0$, 1 and 2 was revealed.[3f] Considering that molecules of **3** and **4** contain five cobalt atoms and the energy level of molecular orbitals produced should be closer than those of tricobalt analogues, it is reasonable that several excited spin states are thermally populated. The EPR spectra of **3** and **4** in CH_2Cl_2 glass at 77 K are silent.

Molecular orbital (MO) interpretation

When the molecular chain of the EMAC is defined as the *z* axis, three types of MO orbitals are generated concerning the M–M bonds. They can be described as follows: σ character MOs are constructed from the overlap of d_{z^2} atomic orbitals, π character MOs are formed from d_{xz} and d_{yz} atomic orbitals and δ character MOs result from the d_{xy} or $d_{x^2-y^2}$ atomic orbitals, depending on the orientation of the *x* and *y* axes. There are two subsets of δ-type orbitals, one with higher energy and metal–ligand anti-bonding character pointing to the direction of four supporting ligands and another with lower energy and orientation of bisecting the adjacent supporting ligands displaying weak interactions with the π orbitals of polypyridyl ligands. All δ-type orbitals are very weak because of the helicity of the spacer ligands and are considered as non-bonding.[11]

Trimetal EMAC is a well-documented system with regards to the molecular calculation of both orbital symmetry and energy levels, and more specifically, substantial work has been carried on tricobalt complexes to understand their spin crossover.[6,7b,11d,e,8] A calculation of the electronic structure for $[Co_3(dpa)_4Cl_2]$ revealed that the molecule possesses a $b^2e^4a_2$ ground state. The SOMO orbital, an orbital of a_2 symmetry, is of metal non-bonding and axial-ligand anti-bonding character and the LUMO is a σ* bonding orbital.

For EMACs containing five metal atoms, the calculation becomes very complicated. Fortunately, a simple calculation of the extended Hückel molecular orbital (EHMO) allows us to make a qualitative analysis of the molecular energy levels and electronic structure of the compound.[11c] The orbital type and corresponding energy levels of MO in the pentacobalt system calculated on $[Co_5(tpda)_4(NCS)_2]$ showed a SOMO of σ non-bonding character (σ^n), similar to that in the tricobalt analogue.[11f,6] The LUMO is a σ anti-bonding orbital (σ*) with an anti-bonding interaction between the σ* of the Co_5 center and the orbital of the axial ligands. The interaction of the ligand orbital with the σ* orbital decreased the σ* energy and thus, stabilized the orbital.

EHMO calculations were performed on **2** by means of the CACAO program (Scheme 5). Both the HOMO and LUMO are σ anti-bonding orbitals (σ*) with an anti-bonding interaction between the σ* of the Co_5 center and the orbital of the axial ligands. Therefore, the LUMO energy levels are strongly at variance with a minor change of axial ligands, which interpreted the significant difference in the magnetic moments between chloro and thiocyanate complexes compared to the nickel and chromium EMACs.[3e] When the compound underwent reduction, the occupancy of an extra electron over the σ* orbital resulted in a weakening of the cobalt–axial ligand interaction and as a consequent, elongated the cobalt–axial bond distances. It is interesting to note that a node of LUMO (σ* orbital 231a) is observed on Co(3), and this is consistent with the elongation of the Co–Co distances on Co(2)–Co(3) and Co(3)–Co(4) bonds upon reduction of **1** and **2**.

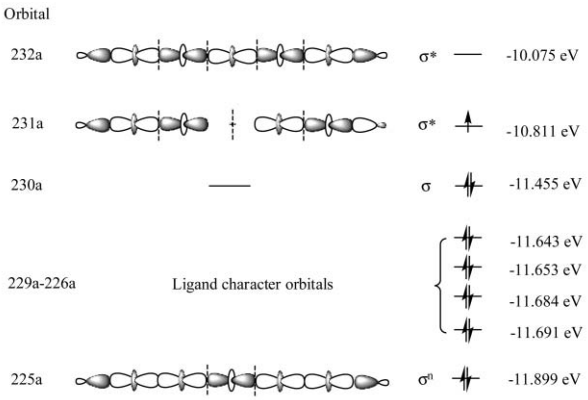

Scheme 5 Sequence of the MOs for **2** calculated from extended Hückel calculations.

As the LUMO energy levels are very sensitive to both supporting and axial ligands, by introducing a more electron-withdrawing substitute, such as pyrazine, a HOMO and LUMO gap high ground state was created, the σ* might decrease relatively and become accessible as they are partly populated and result in a spin equilibrium at room temperature, as was observed for the pyrazine-modulated heptacobalt complexes.[3d] The modulation of the ligand may adjust the electronic structure of the cobalt metal string complexes.

Conclusions

This work introduced the preparation of pentacobalt EMACs $[Co_5(\mu_5\text{-dpzpda})_4X_2]$ (X = Cl^- and NCS^-) with a pyrazine-modulated ligand based on a tripyridyldiamine ligand, *N*,*N*′-di(pyrazin-2-yl)pyridine-2,6-diamine (H_2dpzpda) and their one-electron reduced form $(Ph_4P)[Co_5(\mu_5\text{-dpzpda})_4X_2]$. The structures showed delocalized Co–Co bonds through the whole metal chain in all complexes with Co–Co distances in the range 2.2385(7)–2.2888(15) Å. The distances of inner Co–Co bonds and those of Co–axial ligands became longer after reduction, whereas no significant change was observed for distances of outer Co–Co bonds and Co–N (supporting ligands) bonds. Electrochemical studies on both **1** and **2** were strikingly different to the unmodulated one, exhibiting one reversible oxidation and one

reversible reduction at $E_{1/2}$ = +0.82 and –0.05 V for **1**, and at $E_{1/2}$ = +0.89 and +0.02 V for **2**, respectively. The redox reactions of thiocyanate complex **4** happened at higher potentials than chloride complex **3**. The variable-temperature magnetism of **1–4** was similar to that of heptacobalt EMACs with anomalous magnetic behaviour and a deviation from the Curie–Weiss law. $\chi_M T$ values of 0.53–1.16 emu K mol^{-1} for **1** and **2** in the temperature range 2–300 K suggest a spin equilibrium or a spin-admixture between doublet and quartet states arising from the Boltzmann distribution over different energy levels. Similarly, $\chi_M T$ values of 0.15–0.96 emu K mol^{-1} for **3** and **4** in the temperature range 5–300 K, were obtained, suggesting a spin equilibrium or a spin-admixture between diamagnetic and a triplet state. The results were consistent with the EHMO study, in which the LUMO is a σ anti-bonding orbital (σ*) with an anti-bonding interaction between the σ* of the Co_5 center and the orbital of the axial ligands. This accounts for the elongation of the inner Co–Co bond and Co–axial ligand distances upon gaining an electron, and also implies a sensitivity of the MO energy levels to a minor change of ligands, which may lead to a different thermal distribution. Therefore, it is practical to adjust the electronic structure of cobalt EMACs through the fine-tuning of ligands.

Experimental

Materials

All reagents and solvents were obtained from commercial sources and were used without further purification unless otherwise noted. The CH_2Cl_2 was dried over CaH_2 and freshly distilled prior to use. Tetra-*n*-butylammonium perchlorate (TBAP) was recrystallized twice from ethyl acetate and dried under vacuum.

Physical measurements

Absorption spectra were recorded on a HEWLETT PACKARD 8453 spectrophotometer. IR spectra were performed with a Perkin Elmer FT-IR Spectrometer PARAGON 1000 in the range 400–4000 cm^{-1}. FAB-MS mass spectra were obtained with a JEOL JMS-700 HF double focusing spectrometer operating in the positive ion detection mode. Molar magnetic susceptibility was recorded on a SQUID system with a 2000 Gauss external magnetic field. Electrochemistry was performed with a three-electrode potentiostat (CH Instruments, Model 750A) in CH_2Cl_2 deoxygenated by purging with pre-purified nitrogen gas. Cyclic voltammetry was conducted with the use of a home-made three-electrode cell equipped with a BAS glassy carbon (0.07 cm^2) or platinum (0.02 cm^2) disk as the working electrode, a platinum wire as the auxiliary electrode, and a home-made Ag/AgCl (saturated) reference electrode. The reference electrode is separated from the bulk solution by a double junction filled with electrolyte solution. Potentials are reported *vs.* Ag/AgCl (saturated) and referenced to the ferrocene/ferrocenium (Fc/Fc^+) couple, which occurs at $E_{1/2}$ = +0.54 V *vs.* Ag/AgCl (saturated). The working electrode was polished with 0.03 μm aluminum on Buehler felt pads and was put under ultrasonic radiation for 1 min prior to each experiment. The reproducibility of individual potential values was within ±5 mV. The spectroelectrochemical experiments were accomplished with the use of a 1 mm cuvette, a 100 mesh platinum gauze as the working electrode, a platinum wire as the auxiliary electrode, and a Ag/AgCl (saturated) reference electrode.

Preparation of compounds

N,*N*′-di(pyrazin-2-yl)pyridine-2,6-diamine (H_2dpzpda) was synthesized according to the literature.[9]

[Co_5(μ$_5$-dpzpda)$_4$$Cl_2$] (1). Anhydrous $CoCl_2$ (169 mg, 1.30 mmol), H_2dpzpda (265 mg, 1.00 mmol) and naphthalene (35 g) were placed in an Erlenmeyer flask. The mixture was heated to reflux under argon and then a solution of potassium *tert*-butoxide (235 mg, 2.10 mmol) in *n*-butyl alcohol (5 mL) was added dropwise. The reaction was continued for another 15 h. The product was transferred into hexane to wash out the naphthalene after being cooled, and then 100 mL *ca.* CH_2Cl_2 was used to extract the complex. A brown complex was obtained after evaporation. The single crystals suitable for X-ray diffraction were obtained from diffusion of ether to a chloroform solution. (44 mg, 12% yield), IR (KBr) υ/cm^{-1}: 3417 m, 3087 m, 1586 m, 1493 m, 1471 m, 1418 s, 1348 m, 1156 m, 1028 m, 786 m, 746 m, 468 m. UV-vis (CH_2Cl_2) λ_{max}/nm (ε/dm^3 mol^{-1} cm^{-1}): 234 (7.93×10^4), 281 (9.64×10^4), 343 (9.08×10^4), 538 (2.03×10^4), 768 (7.50×10^3). MS(FAB) *m*/*z* (%): 1419 (20) $[M]^+$, 1382 (10) $[M - Cl]^+$, 1060 (100) $[Co_4(dpzpda)_3Cl]^+$. Elemental analysis (%) $[Co_5(\mu_5\text{-dpzpda})_4Cl_2]\cdot CH_2Cl_2$: calcd. C 42.34, H 2.55, N 26.08; found: C 42.51, H 2.80, N 25.91.

[Co_5(μ$_5$-dpzpda)$_4$(NCS)$_2$] (2). A solution of NaNCS (81 mg, 1 mmol) in CH_3CN (2 mL) was added to a solution of **1** (71 mg, 0.05 mmol) in CH_2Cl_2 (30 mL). The mixture was stirred for 2 d and then filtered. The filtrate was evaporated to dryness, which gave a brown compound. The single crystals suitable for X-ray diffraction were obtained from diffusion of hexane to the CH_2Cl_2 solution. (59 mg, 81% yield), IR (KBr) υ/cm^{-1}: 3424 m, 3092 m, 2915 m, 2040 m, 1586 m, 1494 m, 1470 m, 1421 s, 1347 m, 1156 m, 1029 m, 779 m, 747 m, 468 m. UV-vis (CH_2Cl_2) λ_{max}/nm (ε/dm^3 mol^{-1} cm^{-1}): 233 (1.18×10^5), 279 (1.35×10^5), 341 (1.28×10^5), 528 (2.51×10^4), 749 (6.54×10^3). Elemental analysis (%) $[Co_5(\mu_5\text{-dpzpda})_4(NCS)_2]\cdot CH_2Cl_2\cdot 0.5C_6H_{14}$: calcd. C 43.76, H 2.85, N 26.40; found: C 44.17, H 2.50, N 26.47.

(Ph_4P)[Co_5(μ$_5$-dpzpda)$_4$$Cl_2$] (3). Hydrazine monohydrate ($N_2H_4\cdot H_2O$, 1 mL) was added to a solution of **1** (28 mg, 0.02 mmol) and tetraphenylphosphonium chloride (Ph_4PCl) (12 mg, 0.03 mmol) in CH_2Cl_2 (10 mL). The mixture was stirred for 1 d in an argon atmosphere. Magnesium sulfate was added to remove water and unreacted hydrazine, and then filtered. The single crystals suitable for X-ray diffraction were obtained from diffusion of hexane to the filtrate. (19 mg, 54% yield), IR (KBr) υ/cm^{-1}: 3446 m, 3070 m, 2915 m, 1587 m, 1558 w, 1490 m, 1472 m, 1418 s, 1347 m, 1157 m, 1107 m, 1027 m, 723 m, 689 m, 527 m. UV-vis (CH_2Cl_2) λ_{max}/nm (ε/dm^3 mol^{-1} cm^{-1}): 231 (1.05×10^5), 276 (5.94×10^4), 355 (5.39×10^4), 620 (1.29×10^4), 751 (2.06×10^4). Elemental analysis (%) $(Ph_4P)[Co_5(\mu_5\text{-dpzpda})_4Cl_2]\cdot CH_2Cl_2\cdot C_6H_{14}$: calcd. C 51.68, H 3.76, N 20.33; found: C 51.31, H 3.98, N 19.90.

(Ph_4P)[Co_5(μ$_5$-dpzpda)$_4$(NCS)$_2$] (4). Compound **4** was synthesized using a procedure similar to that for **3**, and the single crystals suitable for X-ray diffraction were obtained from diffusion of

ether to the filtrate. (22.0 mg, 63% yield), IR (KBr) υ/cm^{-1}: 3424 m, 3070 m, 2960 m, 2059 s, 1582 m, 1560 w, 1492 m, 1472 m, 1420 s, 1347 m, 1310 m, 1156 s, 1108 m, 1026 m, 723 m, 689 m, 526 m. UV-vis (CH_2Cl_2) λ_{max}/nm (ε/dm^3 mol^{-1} cm^{-1}): 232 (2.23×10^5), 276 (1.13×10^5), 368 (8.20×10^4), 620 (1.07×10^4), 737 (1.54×10^4). Elemental analysis (%) $(Ph_4P)[Co_5(\mu_5\text{-dpzpda})_4(NCS)_2]\cdot CH_2Cl_2\cdot C_2H_5OC_2H_5$: calcd. C 50.80, H 3.49, N 21.41; found: C 50.48, H 3.72, N 21.04.

Crystal structure determinations†

The chosen crystals were mounted on a glass fiber. Data collection was carried out on a NONIUS Kappa CCD diffractometer at 150(1) K using MoKα radiation (λ = 0.71073 Å) and a liquid nitrogen low-temperature controller. Cell parameters were retrieved and refined using the DENZO-SMN software on all reflections. Data reduction was performed with the DENZO-SMN software. All the structures were solved using SHELXLS-97[12a] and refined with SHELXL-97[12b] by full-matrix least squares on F^2 values. The *R* factors are reasonable and acceptable, in spite of that they are higher than usual because (a) the molecules are large and contain solvent CH_2Cl_2 molecules, which escape quickly during the data collection and (b) some atoms were found in disordered positions in every molecule.

Acknowledgements

The authors acknowledge financial support from the National Science Council and the Ministry of Education of the Republic of China. We are also grateful to Mr Wei-Min Lee for his help with the magnetic measurements.

References

1 (*a*) S.-Y. Lin, I.-W. P. Chen, C.-H. Chen, M.-H. Hsieh, C.-Y. Yeh, T.-W. Lin, Y.-H. Chen and S.-M. Peng, *J. Phys. Chem. B*, 2004, **108**, 959; (*b*) J. F. Berry, F. A. Cotton, L. M. Daniels and C. A. Murillo, *J. Am. Chem. Soc.*, 2002, **124**, 3212; (*c*) I.-W. P. Chen, M.-D. Fu, W.-H. Tseng, J.-Y. Yu, S.-H. Wu, C.-J. Ku, C.-H. Chen and S.-M. Peng, *Angew. Chem., Int. Ed.*, 2006, **45**, 5414.

2 (*a*) J. F. Berry, F. A. Cotton, T. Lu, C. A. Murillo, B. K. Roberts and X. Wang, *J. Am. Chem. Soc.*, 2004, **126**, 7082; (*b*) R. H. Ismayilov, W.-Z. Wang, R.-R. Wang, C.-Y. Yeh, G.-H. Lee and S.-M. Peng, *Chem. Commun.*, 2007, 1121.

3 (*a*) R. Clérac, F. A. Cotton, L. M. Daniels, K. R. Dunbar, K. Kirschbaum, C. A. Murillo, A. A. Pinkerton, A. J. Schutz and X. Wang, *J. Am. Chem. Soc.*, 2000, **122**, 6226; (*b*) C. Y. Yeh, C. H. Chou, K. C. Pan, C. C. Wang, G. H. Lee, Y. O. Su and S. M. Peng, *J. Chem. Soc., Dalton Trans.*, 2002, 2670; (*c*) C.-H. Chien, J.-C. Chang, C.-Y. Yeh, G.-H. Lee, J.-M. Fang and S.-M. Peng, *Dalton Trans.*, 2006, 2106; (*d*) W.-Z. Wang, R. H. Ismayilov, G.-H. Lee, I. P.-C. Liu, C.-Y. Yeh and S.-M. Peng, *Dalton Trans.*, 2007, 830; (*e*) J. F. Berry, F. A. Cotton, T. Lu and C. A. Murillo, *Inorg. Chem.*, 2003, **42**, 4425; (*f*) R. Clérac, F. A. Cotton, K. R. Dunbar, T. Lu, C. A. Murillo and X. Wang, *J. Am. Chem. Soc.*, 2000, **122**, 2272; (*g*) S.-J. Shieh, C.-C. Chou, G.-H. Lee, C.-C. Wang and S.-M. Peng, *Angew. Chem., Int. Ed. Engl.*, 1997, **36**, 56.

4 (*a*) J. F. Berry, F. A. Cotton, P. Lei, T. Lu and C. A. Murillo, *Inorg. Chem.*, 2003, **42**, 3534; (*b*) S.-M. Peng, C.-C. Wang, Y.-L. Jang, Y.-H. Chen, F.-Y. Li, C.-Y. Mou and M.-K. Leung, *J. Magn. Magn. Mater.*, 2000, **209**, 83.

5 (*a*) J. F. Berry, F. A. Cotton, L. M. Daniels, C. A. Murillo and X. Wang, *Inorg. Chem.*, 2003, **42**, 2418; (*b*) J. F. Berry, F. A. Cotton, P. Lei and C. A. Murillo, *Inorg. Chem.*, 2003, **42**, 377.

6 M.-M. Rohmer, I. P.-C. Liu, J.-C. Lin, M.-J. Chiu, C.-H. Lee, G.-H. Lee, M. Bénard, X. López and S.-M. Peng, *Angew. Chem., Int. Ed.*, 2007, **46**, 3533.

7 (*a*) S.-J. Shieh, C.-C. Lin, I. Chao, C.-C. Wang and S.-M. Peng, *Chem. Commun.*, 1996, 315; (*b*) C.-K. Kuo, I. P.-C. Liu, C.-Y. Yeh, C.-H. Chou, T.-B. Tsao, G.-H. Lee and S.-M. Peng, *Chem.–Eur. J.*, 2007, **13**, 1442.

8 (*a*) D. A. Pantazis and J. E. McGrady, *J. Am. Chem. Soc.*, 2006, **128**, 4128; (*b*) M.-M. Rohmer and M. Bénard, *J. Am. Chem. Soc.*, 1998, **120**, 9372; (*c*) M.-M. Rohmer, A. Strich, M. Bénard and J.-P. Malrieu, *J. Am. Chem. Soc.*, 2001, **123**, 9126; (*d*) M.-M. Rohmer and M. Bénard, *J. Cluster Sci.*, 2002, **13**, 333.

9 R. H. Ismayilov, W.-Z. Wang, G.-H. Lee and S.-M. Peng, *Dalton Trans.*, 2006, 478.

10 C.-Y. Yeh, C.-C. Wang, Y.-H. Chen and S.-M. Peng, in *Redox Systems Under Nano-Space Control*, ed. T. Hirao, Springer, Germany, 2006, ch. 5.

11 (*a*) X. López, M.-Y. Huang, G.-C. Huang, S.-M. Peng, F.-Y. Li, M. Bénard and M.-M. Rohmer, *Inorg. Chem.*, 2006, **45**, 9075; (*b*) N. Benbellat, M.-M. Rohmer and M. Bénard, *Chem. Commun.*, 2001, 2368; (*c*) J. F. Berry, F. A. Cotton, L. M. Daniels, C. A. Murillo and X. Wang, *Inorg. Chem.*, 2003, **42**, 2418; (*d*) P. Kiehl, M.-M. Rohmer and M. Bénard, *Inorg. Chem.*, 2004, **43**, 3151; (*e*) M. Bénard, J. F. Berry, F. A. Cotton, C. Gaudin, X. López, C. A. Murillo and M.-M. Rohmer, *Inorg. Chem.*, 2006, **45**, 3932; (*f*) C.-C. Wang, W.-C. Lo, C.-C. Chou, G.-H. Lee, J.-M. Chen and S.-M. Peng, *Inorg. Chem.*, 1998, **37**, 4059.

12 (*a*) G. M. Sheldrick, *SHELXS-97, Program for solution of crystal structures*, University of Göttingen, Germany, 1997; (*b*) G. M. Sheldrick, *SHELXL-97, Program for refinement of crystal structures*, University of Göttingen, Germany, 1997.

